Micromagnetic simulation on the dynamic susceptibility spectra of cobalt nanowires arrays: the effect of magnetostatic interaction*

Chen Wen-Bing(陈文兵),   Han Man-Gui(韩满贵)[†],   Zhou Hao(周 浩),

Ou Yu(欧 雨), and Deng Long-Jiang(邓龙江)

State Key Laboratory of Electronic Thin Films and Integrated Devices, University of Electronic Science and Technology of China, Chengdu 610054, China

Micromagnetic simulations have been performed to obtain the dynamic susceptibility spectra of 4×4 cobalt nanowire arrays with different spatial configurations and geometries. The susceptibility spectra of isolated wires have also been simulated for comparison purposes. It is found that the susceptibility spectrum of nanowire array bears a lot of similarities to that of an isolated wire, such as the occurrences of the edge mode and the bulk resonance mode. The simulation results also reveal that the susceptibility spectrum of nanowire array behaves like that of single isolated wire as the interwire distance grows to an extent, which is believed due to the decrease of magnetostatic interaction among nanowires, and can be further confirmed by the static magnetic hysteresis simulations. In comparison with single nanowire, magnetostatic interaction may increase or decrease the resonance frequencies of nanowire arrays assuming a certain interwire distance when the length of array increases. Our simulation results are also analysed by employing the Kittel equation and recent theoretical studies.

Keywords: micromagnetic simulation, dynamic susceptibility, nanowire array, magnetostatic interaction

PACC: 7540G, 7540M, 3240, 7500

1. Introduction

The potential applications of magnetic nanowire (NW) arrays in perpendicular magnetic recording industry and microwave devices have stimulated numerous researches to investigate their static and dynamic magnetic properties.[1−13] However, the tendency to reduce the dimension of NW arrays and their constituents gives rise to a new problem: magnetostatic interaction among NWs, which plays a crucial role especially when the separation between adjacent NWs is greatly shortened. Many works have pointed out that the static magnetic properties of NWs are affected by magnetostatic interaction between NWs. For instance, it has been shown that strong magnetostatic interaction in magnetic NW arrays could lead to an antiferromagnetic ground state (checkerboard pattern)[4−6] and the magnetostatic interaction field in low aspect ratio CoP cylinder nanoarrays is strong enough to exceed the switching field of the elements in the arrays.[7] Recent studies on the magnetization reversal behaviour of high density cobalt NW arrays reveal that the magnetostatic interaction field between NWs increases not only with NW diameters but also with NW lengths.[8]

A second facet concerning magnetic NW arrays is their dynamic properties. Among them, the dynamic susceptibility spectrum of NW arrays is of great importance in both fundamental and application fields. One attribute that makes this property desirable is that the eddy current loss interfering with susceptibility spectrum is greatly suppressed for nanowires.[9−11] Another reason is that the resonance frequency of the uniform gyromagnetic mode for NW arrays can be tuned by varying the aspect ratio and material, applying dc fields, and changing the porosity of membranes in which NWs are embedded.[12] The last method is thoroughly discussed in Refs. [12] and [13], indicating that dipolar interaction between NWs has a great impact on the resonance frequency of NW array.

As an important technique to investigate the dynamic properties of nanostructured materials,[14−25] micromagnetics is fueled by the growing calculation speed of computers. However, the simulation on NW

arrays still requires prohibitive time,[3,21] resulting in the neglect of the dynamic properties of NW arrays in the arena of micromagnetics. Previous simulations on dynamic susceptibility focused mainly on isolated elements such as single nanowire,[14,15] films,[22] nanodots.[23] Other simulations concentrate on coupled systems such as coupled stripes,[16] submicron arrays,[17] and nanodot arrays,[18−20] indicating that magnetostatic interaction is a dominant factor in the dynamic magnetic properties of these systems.

Enlightened by the above-mentioned experiments and micromagnetic simulations, this work is intended to investigate the susceptibility spectra arising from cobalt NW arrays with different spatial configurations and geometries by means of numerical simulation. The aim is to qualitatively analyse the contributions of magnetostatic interaction in NW array with different configurations. To this end, the magnetic behaviours of isolated wires have also been studied for comparison purposes and the interwire distance between neighbouring wires in the array is deliberately set to be larger than exchange length $L_{ex} = \sqrt{2A/\mu_0 M_s^2} \approx 4.93$ nm so that exchange coupling between wires could not enter our investigation.

2. Simulation procedure

The micromagnetic simulations are performed using a three-dimensional object-oriented micromagnetic framework (OOMMF)[26] by solving the Landau–Lifshitz–Gilbert (LLG) equation as a function of time:

$$\frac{dM}{dt} = -\gamma M \times H_{eff} + \frac{\alpha}{M_s}\left(M \times \frac{dM}{dt}\right), \qquad (1)$$

where M is the magnetization and H_{eff} is the effective field taking into account the exchange, self-magnetostatic, anisotropy and applied field terms; γ (2.21×10^5 mA$^{-1}\cdot$S^{-1}) is the Gilbert gyromagnetic ratio and α (damping constant) is set at 0.015 and 0.5 for the dynamic response of the applied field and hysteresis loop simulation, respectively.

In our work, the field-dependent behaviours of single isolated cobalt NWs, assuming a cylindrical shape, and their corresponding 4×4 square NW arrays are simulated. This choice is justified by previous works pointing out that the simulation results of 4×4 NW arrays agree well with experimental values.[3,27] For simplicity, the diameters of all nanowires in the simulations are fixed at 40 nm. The simulated NW arrays fall into two categories: the one with varying interwire-distance (D) and the one with a fixed D but with varying length (L). The default parameters in OOMMF for cobalt are taken in our simulations: saturation magnetization $M_s = 14 \times 10^5$ A/m, exchange stiffness constant $A = 30 \times 10^{-12}$ J/m, anisotropy constant $K_1 = 5.2 \times 10^5$ J/m^3. The magnetocrystalline anisotropy easy axis is set to be the [001] direction, parallel to the wire length (z-direction). The initial magnetization is along the [100] direction and normal to the wire length. And a cubic cell size of 5 nm is adopted for all simulations.

The magnetic spectra of NWs are obtained in the following procedure. Firstly, starting from the initial magnetization, the equilibrium configuration of magnetization is obtained in the absence of external-applied magnetic field. Then a weak pulse field assuming the form of $H(t) = 1000\exp(-10^9 t)$ (t in s, H in A/m) is applied perpendicular to the long axis of the wires. The dynamic response of magnetization is tracked under the pulse field. Both the pulse field and excited magnetization are then processed by a fast Fourier transform (FFT) approach, after which the susceptibility spectrum $\chi(\omega)$ are calculated using the following equation

$$\chi(\omega) = M(\omega)/H(\omega) = \chi'(\omega) - i\chi''(\omega), \qquad (2)$$

where ω is the frequency, $M(\omega)$ and $H(\omega)$ are the expressions in frequency domain for magnetization and pulse field after FFT treatment, respectively; $\chi'(\omega)$ refers to the real part of $\chi(\omega)$ and $\chi''(\omega)$ denotes the imaginary part.

The frequency corresponding to the maximum value of $\chi''(\omega)$ is the so-called resonance frequency, which can be examined by the Kittel equation when the magnetocrystalline anisotropy easy axis is along the wire length[28]

$$\omega = \frac{\gamma}{2\pi}\sqrt{[H_0 + H_k + (N_x - N_z)M_z][H_0 + H_k + (N_y - N_z)M_z]}, \qquad (3)$$

where H_0 is the external static field, $H_k = 2K_1/\mu_0 M_s$ is the effective magnetocrystalline anisotropy field, N_x, N_y, N_z are the demagnetizing factors depending on the ratio of ellipsoidal axes.

3. Results and discussion

The obtained equilibrium configuration for an NW array with $D = 50$ nm is shown in Fig. 1. The three-dimensional (3D) image of the magnetization configurations for the NW array typifies a "checkerboard" pattern while each wire retains a flower state. In order to minimise the total free energy of the system, magnetizations between the nearest neighbours are aligned antiparallelly, and form a closure pattern at the ends. As indicated by the checkerboard signature observed in the MFM images of the remanent state for nanomagnet arrays,[4,5] magnetization configuration shown in Fig. 1 is a macroscopic manifestation of the strong magnetostatic interactions between wires. We believe that this antiferromagnetic alignment between adjacent NWs also has to do with the initial magnetization of the NW array, which is set to be normal to the wire length. In Refs. [27] and [29], similar observations were obtained in Ni NW array and elliptical NiFe nanoarray, respectively.
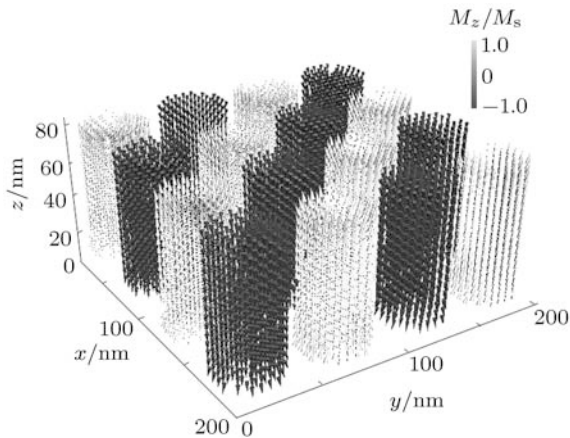

Fig. 1. Magnetization configurations in the equilibrium state for a cobalt 4×4 NW array, with $D = 50$ nm (centre-to-centre distance) and $L = 80$ nm. Each wire has a diameter of 40 nm.

Intuitively, magnetostatic interaction between wires would decay as D increases. This is substantiated by our simulation. Illustrated in Fig. 2 is the equilibrium configuration for the NW arrays with a larger D ($D = 240$ nm) than that in Fig. 1. Clearly, magnetizations for all wires are parallel and the checkerboard pattern vanishes. This configuration indicates that the wires in the array are weakly influenced by each other as the interwire coupling is greatly weakened by the large spacing. Thus it is predictable that the NW array with equilibrium configuration in Fig. 2 would behave rather like single isolated wire.
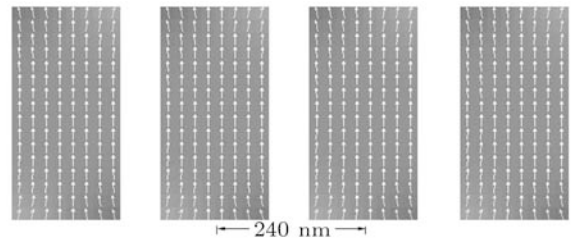

Fig. 2. Magnetization configurations (cross section of xz plane) in the equilibrium state for a cobalt 4×4 NW array with $D = 240$ nm, $L = 80$ nm. Each wire has a diameter of 40 nm.

Further attesting the magnetostatic interaction among NWs are the hysteresis loops, as shown in Fig. 3, for single wire and the aforementioned NW arrays. The hysteresis loop for NW array with $D = 50$ nm is greatly sheared due to the interaction among wires, showing decreased squareness and coercivity. The decrease in coercivity is around 2000 Oe (1 Oe=79.5775 A/m), nearly a third of the coercivity for NW array with $D = 240$ nm. The sheared hysteresis loops for NW arrays had been experimentally observed.[8,12] According to the phenomenological mean field theory,[12] we believe that the smaller coercivity values can be explained by an interaction field perpendicular to the wire axis, which would decrease the total effective field by competing against the shape anisotropy and magnetocrytalline anisotropy that favour an easy axis along the wire length.
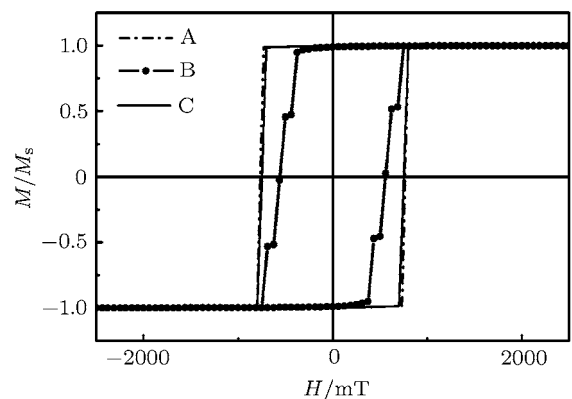

Fig. 3. M–H loops for an isolated single NW (A, dot-dashed line) with $L = 80$ nm, and for its 4×4 NW array with $D = 50$ nm (B, marked by full circles) and $D = 240$ nm (C, straight line) respectively. The magnetic field is applied along the length direction of NW.

As a result, a lower external field can switch the magnetic moment in the NW array with $D = 50$ nm. Besides, multiple Barkhausen jumps observed in the hysteresis loop of NW array with $D = 50$ nm are believed to stem from the magnetostatic interaction between

wires and the non-synchronous magnetization reversal process for different wires in the array.[30] Also clearly shown in Fig. 3, the hysteresis loop for NW array with $D = 240$ nm is very close to that of an isolated single wire, which is in accordance with its equilibrium magnetization configuration shown in Fig. 2.

The magnetic spectra for the above-mentioned NW arrays are shown in Fig. 4. For comparison, the magnetic spectrum for a single isolated wire is also illustrated. Similar to the magnetic spectrum
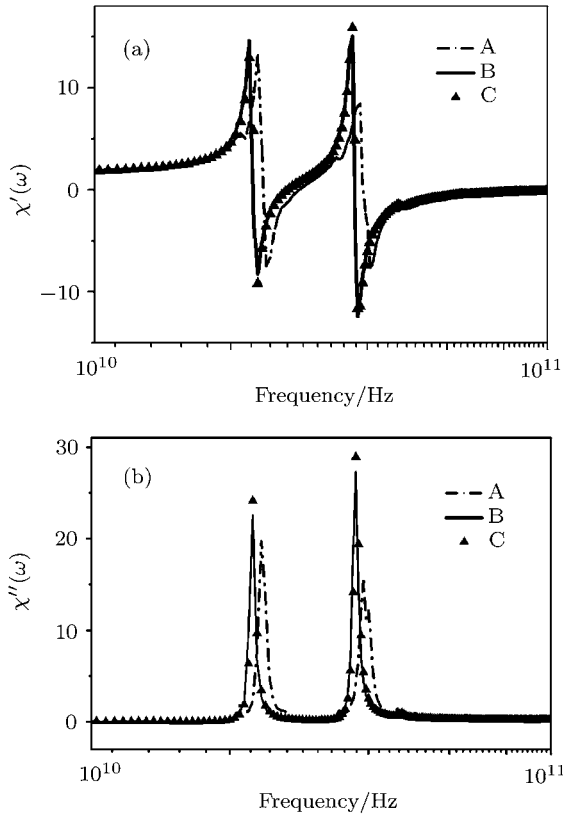

Fig. 4. Real (a) and imaginary (b) susceptibility spectrum for NW array with $L = 80$ nm, $D = 50$ nm (A, marked by dashed line) and $D = 240$ nm (B, straight line). The imaginary susceptibility spectrum for single NW with $L = 80$ nm is also plotted (C, marked by triangle).

of a single wire, there are two resonance peaks for the NW arrays. Both peaks can be ascribed to the natural resonance of the spins in the NW, but they are caused by different parts of the wires' magnetization. As discussed in other previous work,[14,15,31] the peak at the lower frequency (called edge mode or rim mode) is caused by the splay pattern of the edge spin configuration, while the one at the high frequency (called the bulk resonance mode or main mode) is due to the spin configuration in the middle part of the wires. Both the edge mode and the bulk mode have been confirmed by the experiments in thin ellipsoidal

magnetic elements[32] and in cobalt stripes.[33] Other modes observed in these experiments correspond to the minor peaks around the two main peaks, arising from the inhomogeneity of the magnetization configuration, which is partly demonstrated in Fig. 1.

Moreover, in Fig. 4, the magnetic spectrum shifts in frequency as D changes. The magnitudes of both major peaks also are observed to vary, which is believed due to the change of relative volumes of the end parts and central parts of the wires. The extent of the end parts is mainly determined by the self-magnetostatic field at the wire ends.[15] In our case, this field for one wire in the array is influenced by the stray field from neighbouring wires due to magnetostatic interaction, which would change as D enlarges. In the mean time, the effective field that determines the volume of the central part is also affected by magnetostatic interaction, but in a different manner and to a different extent. Consequently, the change of the relative magnitudes of the two major peaks is expected.

In line with the equilibrium magnetization configurations and hysterisis loops, the magnetic spectrum of NW array (Fig. 4) with $D = 240$ nm behaves like that of single isolated wire. This behaviour can also be observed in the magnetic spectra (not shown here) of NW array with $L = 200$ nm and varying D. In Figs. 5(a) and 5(b), the bulk resonance frequencies as functions of D for the two sets of NW arrays are plotted. In both cases, as D becomes larger, the resonance frequency would approach to that of single isolated wire (37.6 GHz for the wire with $L = 80$ nm and 42.97 GHz for the wire with $L = 200$ nm).

We can understand the above phenomena by employing recently published research results on the magnetostatic interaction between NWs. In Ref. [34], an explicit form of the interaction energy E_{int} between two nanotubes with axial magnetization was obtained. Applied to a pair of NWs, the interaction energy E_{int} reads

$$E_{\text{int}} = -\frac{\sigma_1 \sigma_2 \pi \mu_0 M_s R^4}{2d}[(1 + (L/d)^2)^{-1/2} - 1], \quad (4)$$

where the unit of E_{int} is J, σ_1, σ_2 takes the value ± 1, allowing the magnetization of each NW to point up or down; M_s is saturation magnetization of each wire, R the radius, L the length, d the distance between NWs. This equation is suitable for two NWs in the array studied here since in equilibrium state magnetization is parallel to the wire axis and only deviates slightly from the equilibrium state when perturbed by the external pulse field. Exploiting this formula, the abso-

lute value of interaction energy for two adjacent NWs embedded in the NW array as described in Fig. 5(a) or 5(b) is demonstrated in Fig. 5(c). It is evident that the interaction energy between two neighbouring NWs decreases rapidly as D increases. For example, when the distance between the two NWs with diameter of 40 nm and $L = 80$ nm reaches 240 nm, the interaction energy between them would decrease to a value near zero. With little interaction between NWs, the resonance frequency of NW array would approach that of single NW, as shown in Figs. 5(a) and 5(b).
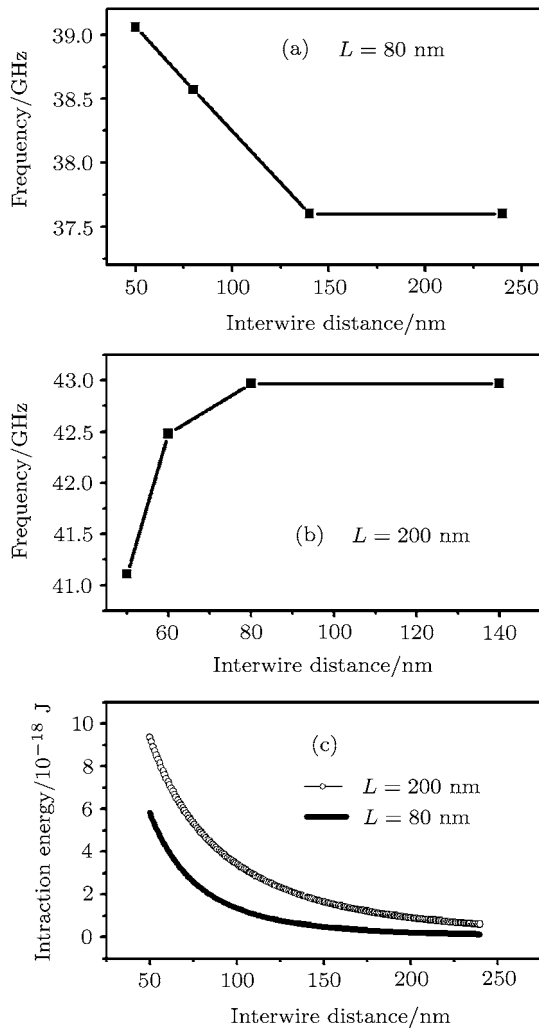

Fig. 5. The dependence of resonance frequency on interwire distance D for 4×4 array with $L = 80$ nm in (a) and $L = 200$ nm in (b). The dependence of interaction energy on D for two adjacent NWs embedded in the two sets of arrays is shown in (c).

In order to investigate the effect of L on the susceptibility spectra, the behaviours of another set of nanowire arrays with a fixed $D = 80$ nm and varying L from 60 nm to 800 nm have been simulated. Three of them are shown in Fig. 6. Clearly shown is that the bulk mode of nanowire arrays shifts up to the higher frequency as L increases, while the position of edge mode remains almost unaffected. The relative magnitudes of the high frequency peak and low frequency peak increase as L grows, reflecting the growing middle part of the wires and the almost fixed regions at the end of the wires. Similar behaviours have also been observed in Ref. [15].
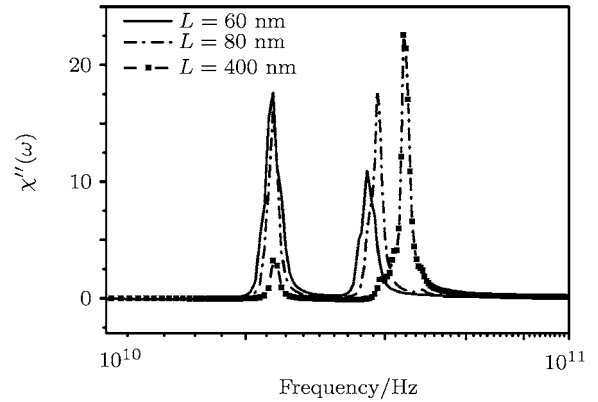

Fig. 6. The imaginary susceptibility spectrum of NW arrays with a fixed $D = 80$ nm but with different length L.

Shown in Fig. 7(a) are the bulk mode frequencies of single NW with different aspect ratio (length/diameter) ranging from 1.5 to 20, and the resonance frequencies for their corresponding 4×4 NW arrays with $D = 80$ nm. The calculated values based on the Kittel's equation (see Eq. (3)) are also shown (see the dotted-dash line). Although the resonant frequencies for both the single NW and NW array approach the Kittel prediction as L increases, the difference between the frequencies of single NW and those of NW arrays could not be overlooked. When L is shorter than 200 nm, the resonance frequency of NW array is lower than that of single NW. This situation is reversed after L exceeds 400 nm.

Equation (4) may help us gain some insight into the difference in Fig. 7(a). Based on Eq. (4), figure 7(b) shows the absolute value of interaction energy as a function of L for two adjacent NWs embedded in the array as described by Fig. 7(a). It is evident that the interaction energy between neighbouring wires increases as L increases. Meanwhile, the shape anisotropy field favouring an easy axis along the long axis also increases. This can be seen in Fig. 7(a) as guided by the dot-dashed line since the frequency increase in the Kittel equation (Eq. (3)) is contributed mainly by the increase in

shape anisotropy as the length becomes larger. Eventually, it is the relation between magnetostatic interaction and the sum of shape anisotropy and axial magnetocrystalline anisotropy that leads to the increasing resonance frequency trend for NW array as L rises up. Generally speaking, when L is shorter than 200 nm, magnetostatic interaction between NW arrays could augment anisotropy along the wire length and increase the resonance frequency. The same analysis can be applied to Fig. 5(a).
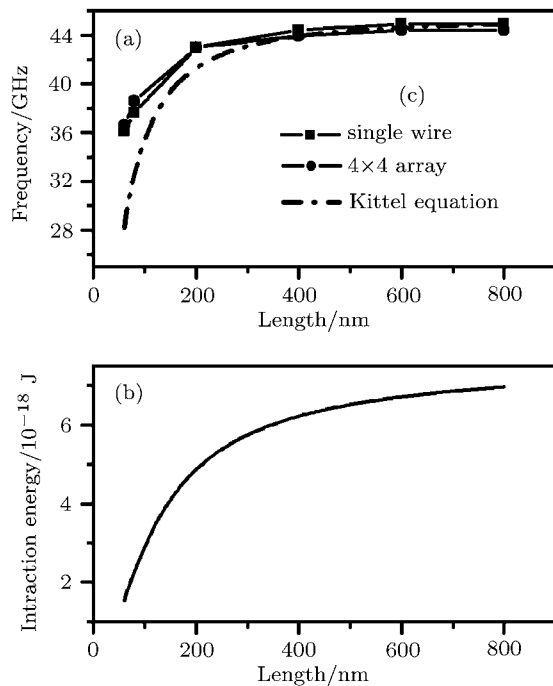

Fig. 7. (a) The variation of resonance frequency for NW arrays as a function of length L. The resonance frequencies for isolated wires are also plotted for comparison. Calculation based on Kittel equation (Eq. (3)) is shown by the dot-dashed line. The dependence of interaction energy on L between two neighboring NWs embedded in the NW array is shown in (b).

But when L is larger than 400 nm, magnetostatic interaction can diminish shape anisotropy and magnetocrystalline anisotropy, resulting in lower resonance frequencies than those in single NW. The latter trend agrees with previous theoretical and experimen-tal results.[12,16] We suppose that this is because both the theoretical and experimental results address only nanowires with large aspect ratio. Quantitative solution to this problem is very complex since it requires detailed knowledge about the interaction field experienced by each wire in the array and about how it affects the total effective field; even recent theoretical attempts to gain detailed information about the magnetostatic interaction field in coupled systems are confined to only a few wires.[34,35] Magnetic susceptibility measurements and ferromagnetic resonance experiments on NW arrays with different L would help clarify this problem, which are under way based on the above simulation results.

4. Conclusion

Micromagnetic simulations have been performed to obtain the magnetic susceptibility spectra for 4 × 4 cobalt NW arrays with varying interwire distances and lengths. Many similarities have been found, in the occurrence of edge mode and bulk resonant mode, between the susceptibility spectra of NW arrays and that of an isolated wire. The susceptibility spectrum of an NW array will behave much like that of an isolate NW when the interwire distance increases to an extent, which is attributed to the decreased magnetostatic interaction among NWs in the array. This has been further confirmed by the M–H loop simulations. When the length of NW array with $D = 80$ nm increases, magnetostatic interaction first increases the resonance frequency when the length is shorter than 200 nm and then decreases the resonance frequency after the length exceeds 400 nm.

Acknowledgment

References

[1] Xiao J J, Sun C, Xue D S and Li F S 2001 *Acta Phys. Sin.* **50** 1605 (in Chinese)

[2] Guo Z Z and An C H 2008 *Chin. Phys. Lett.* **12** 4406

[3] Gao J H, Sun D L, Zhan Q F, He W and Cheng Z H 2007 *Phys. Rev.* B **75** 064421

[4] Hwang M, Abraham M C, Savas T A, Smith H I, Ram R J and Ross C A 2000 *J. Appl. Phys.* **87** 5108

[5] Nielsch K, Wehrspohn R B, Barthel J, Kirschner J, Gösele U, Fischer S F and Kronmüller H 2001 *Appl. Phys. Lett.* **79** 1360

[6] Ross C A, Hwang M, Shima M, Cheng J, Farhoud Y M, Savas T A, Smith H I, Schwarzacher W, Ross F M, Redjdal M and Humphrey F B 2002 *Phys. Rev.* B **65** 144417

[7] Shima M, Hwang M and Ross C A 2003 *J. Appl. Phys.* **93** 3440

[8] Kartopu G, Yalcín O, Es-Souni M and Başaran A C 2008 *J. Appl. Phys.* **103** 093915

[9] Gao B, Qiao L, Wang J B, Liu Q F, Li F S, Feng J and Xue D S 2008 *J. Phys.* D: *Appl. Phys.* **41** 235005

[10] Qiao L, Han X H, Gao B, Wang J B, Wen F S and Li F S 2009 *J. Appl. Phys.* **105** 053911

[11] Ledieu M, Schoenstein F, Le Gallou J H, Valls O, Queste S, Duverger F and Acher O 2003 *J. Appl. Phys.* **93** 7202

[12] Encinas-Oropesa A, Demand M, Piraux L, Huynen I and Ebels U 2001 *Phys. Rev.* B **63** 104415

[13] Encinas-Oropesa A, Demand M, Piraux L, Ebels U and Huynen I 2001 *J. Appl. Phys.* **89** 6704

[14] Liu R L, Wang J B, Liu Q F, Wang H X and Jiang C G 2008 *J. Appl. Phys.* **103** 013910

[15] Dao N, Donahue M J, Dumitru I, Spinu L, Whittenburg S L and Lodder J C 2004 *Nanotechnology* **15** S634

[16] Gérardin O, Youssef J B, Le Gall H, Vukadinovic N, Jacquart P M and Donahue M J 2000 *J. Appl. Phys.* **88** 5899

[17] Dantas C C and Andrade L A 2008 *Phys. Rev.* B **78** 024441

[18] Gubbiotti G, Madami M, Tacchi S, Carlotti G and Okuno T 2006 *J. Appl. Phys.* **99** 08C701

[19] Keatley P S, Kruglyak V V, Neudert A, Galaktionov E A and Hicken R J, 2008 *Phys. Rev.* B **78** 214412

[20] Kruglyak V V, Keatley P S, Hicken R J, Childress J R and Katine J A 2006 *J. Appl. Phys.* **99** 08F306

[21] Camley R E, McGrath B V, Khivintsev Y, Celinski Z, Adam R, Schneider C M and Grimsditch M 2008 *Phys. Rev.* B **78** 024425

[22] Vukadinovic N, Vacus O, Labrune M, Acher O and Pain D 2000 *Phys. Rev. Lett.* **85** 2817

[23] Vukadinovic N and Boust F 2007 *Phys. Rev.* B **75** 014420

[24] Chen R J, Zhang H W, Shen B G, Yan A R and Chen L D 2009 *Chin. Phys.* B **18** 2582

[25] Song S Y, Guo G H, Zhang G F and Song W B 2009 *Acta Phys. Sin.* **58** 5757 (in Chinese)

[26] Donahue M J and Porter D G 2002 *OOMMF User's Guide*, Version 1.2a3 (http://math.nist.gov/oommf)

[27] Hertel R 2001 *J. Appl. Phys.* **90** 5752

[28] Kittel C 1948 *Phys. Rev.* **73** 155

[29] Scholz W, Suess D, Schrefl T and Fidler J 2002 *J. Appl. Phys.* **91** 7047

[30] Velázquez J, García C, Vázquez M and Hernando A 1999 *J. Appl. Phys.* **85** 2768

[31] Gérardina O, Le Gall H, Donahue M J and Vukadinovic N 2001 *J. Appl. Phys.* **89** 7012

[32] Guyader L L, Anceau C, Kirilyuk A, Rasing T, Berkov D and Bär L 2006 *Phys. Rev.* B **73** 060402(R)

[33] Meckenstock R, Barsukov I, Posth O, Lindner J, Butko A and Spoddig D 2007 *Appl. Phys. Lett.* **91** 142507

[34] Escrig J, Allende S, Altbir D and Bahiana M 2008 *Appl. Phys. Lett.* **93** 023101

[35] Beleggia M, Tandon S, Zhu Y and Graef M D 2004 *J. Magn. Magn. Mater.* **278** 270